Columbia University in the City of New York

LAMONT GEOLOGICAL OBSERVATORY

PALISADES, NEW YORK

MEASUREMENT OF P AND S SOUND VELOCITIES UNDER PRESSURE ON LABORATORY MODELS OF THE EARTH'S MANTLE

Orson L. Anderson and Edward Schreiber

Contract No. AF-AFOSR 49(638)-1355

Project No. 4810 & 3810 - Task 8652

Final Report

Period Covered: 16 December 1963 - 15 December 1965

16 December 1965

Prepared for

AIR FORCE OFFICE OF SCIENTIFIC RESEARCH
OFFICE OF AEROSPACE RESEARCH
UNITED STATES AIR FORCE
WASHINGTON, D. C.

Sponsored by

ADVANCED RESEARCH PROJECTS AGENCY

ARPA Order No. 292-63, 292-64

TABLE OF CONTENTS

TABLE OF CONTENTS (continued)

LIST OF TABLES

LIST OF FIGURES

ABSTRACT. The techniques of ultrasonic interferometry were used to measure the isotropic sound velocities and their derivatives for polycrystalline specimens of aluminum oxide and magnesium oxide. The pressure derivatives were determined to 4 kbars at room temperature and at the -78.5°C. The temperature derivatives were measured at 1 atmosphere. The velocities and their derivatives at room temperature are

	MgO	Al_2O_3	
v_p	9.7711	10.845	km/sec
v_s	5.9682	6.3730	km/sec
dv_p/dP	7.711×10^{-3}	5.175×10^{-3}	km/sec/kbar
dv_s/dP	4.351×10^{-3}	2.207×10^{-3}	km/sec/kbar
dv_p/dT	-5.0×10^{-4}	-3.7×10^{-4}	km/sec/°C
dv_s/dT	-4.8×10^{-4}	-3.1×10^{-4}	km/sec/°C

The isothermal pressure derivatives of the bulk modulus were determined to be $(dB_T/dP)_{MgO} = 3.94$ and $(dB_T/dP)_{Al_2O_3} = 3.99$ at room temperature.

From these data, the critical temperature gradient for velocities, $(dT/dP)_v$, were evaluated, and the velocity behavior of these materials as a function of temperature and depth in the mantle are discussed. It was found that, because $(dT/dP)_{v_p} > (dT/dP)_{v_s}$, they exhibit a shear velocity minimum and a less pronounced longitudinal velocity minimum under conditions likely to exist in the upper mantle.

An expression was derived, employing the measured values of the bulk modulus B_o and its pressure derivative B_o', which predicts compression at extremely high pressures. Using the derived expression

$$\ln(V_o/V) = (1/B_o') \ln [B_o'(P/B_o) + 1]$$

and the values of B_o and B_o' for MgO and Al_2O_3 reported here, the agreement between the calculated compression and measured compression reported in the literature was within 0.5% to 350 kilobars.

I. INTRODUCTION

The objective of this research program was to undertake investigation of the behavior of the pressure and temperature derivatives of homogeneous mineral specimens; the data obtained are applicable to the resolution of questions regarding the behavior of seismic velocities in a homogeneous mantle. Some of the problems to which results of these studies apply are the lateral variations of velocity at constant depth; variation of seismic velocities with depth; dispersion of seismic velocities with temperature; and, finally, the problem of the 'shadow zone' phenomenon in the upper mantle.

The program differs from the usual experiments on the sound velocity in rocks in several ways. First, the materials employed were synthetically prepared polycrystalline mineral specimens. The specimens were prepared in a manner so that they were of essentially zero porosity and controlled (small) grain size. Second, the technique used for the measurement of the sound velocities and their derivatives was ultrasonic interferometry, which permitted accurate determination of the velocity derivatives in the P-T plane. This accuracy was sufficient to permit the calculation of the compression of the material well beyond the range of the actual measurements.

Investigations on the behavior of rock specimens have taken two approaches. These are the direct measurement of velocity with pressure or temperature;[1,2,3] or the direct measure of the compressibility.[4] In both instances the presence of pores, cracks, and mineral orientations complicate the results. Typically, the initial slopes represent extrinsic rather than intrinsic effects; the 1 atm velocities or compressibilities are obtained by extrapolating back from higher pressure data where the intrinsic behavior is observed. Further, the techniques are generally not sufficiently accurate to define the pressure derivatives. Temperature measurements on rocks suffer the further disadvantage of the irreversible chemical changes within the rock when it is heated, so that low temperature measurements would not correspond to high temperature measurements on the same materials. Measurements on mono-mineral specimens of extremely good quality do not suffer these disadvantages. In particular, intrinsic properties are measured over the entire experimental range, and with surficient accuracy to define the derivatives. Thus, the results of these experiments leads to precise numerical data applicable to the propagation of sound velocity and the elastic properties within the earth.

II. ACCOMPLISHMENTS

We have measured the velocities and their pressure and temperature derivatives of two polycrystalline specimens, one of MgO and the other Al_2O_3. The results have been published in a series of papers and their applicability to the problems of the deep earth discussed. Analytic methods for computing the compression and velocities at extremely high pressures, employing the data obtained at relatively low pressure were developed. In all, ten papers were produced. Seven have been published, two have been accepted and are in press, and one has been submitted. The titles of these papers are listed below. Abstracts of these papers appear in Appendix A.

A. Papers published:

1. "Conditions for a Density Minimum in the Upper Mantle," O. L. Anderson, J. Geophys. Res., 70[6], 1457-1461, 1965.

2. "The Relation between Refractive Index and Density of Minerals Related to the Earth's Mantle," O. L. Anderson and E. Schreiber, J. Geophys. Res., 70[6], 1463-1471, 1965.

3. "Lattice Dynamics in Geophysics," O. L. Anderson, Trans. N.Y. Acad. Sci., Ser. II, 27[3], 298-308, 1965.

4. "The Bulk Modulus-Volume Relationship for Oxide Compounds and Related Geophysical Problems," O. L. Anderson and J. E. Nafe, J. Geophys. Res., 70[16], 3951-3963, 1965.

5. "An Approximate Method of Estimating Shear Velocity from Specific Heat," O. L. Anderson, (Letter) J. Geophys. Res., 70[18], 4726-4728, 1965.

6. "The Pressure Derivative of the Sound Velocities of Polycrystalline Magnesia," O. L. Anderson and E. Schreiber, J. Geophys. Res., 70[20], 5241-5248, 1965.

7. "Two Methods for Estimating Compression and Sound Velocity at Very High Pressures," Proc. Nat. Acad. Sci., 54[3], 667-673, 1965.

B. Papers accepted for publication:

1. "The Pressure Derivatives of the Sound Velocities of Polycrystalline Alumina," E. Schreiber and O. L. Anderson, J. Am. Ceram. Soc., in press.

2. "Seismic Parameter ϕ: Computation at Very High Pressure from Laboratory Data," O. L. Anderson, Bull. Seism. Soc. Am., in press.

C. Papers submitted:

1. "Temperature Dependence of the Velocity Derivatives of Periclase," E. Schreiber and O. L. Anderson.

III. MEASUREMENTS AND RESULTS

A. Specimens

A specimen of hot-pressed magnesium oxide was obtained from the ceramics laboratory at the University of California at Berkeley. This material was 99.9% theoretical density. The aluminum oxide (lucalox) was obtained from the General Electric Company. This specimen had a density that was 99.75% of theoretical. The specimens were prepared by having two basal surfaces ground and polished parallel to within 0.0001" per inch and flat to within 0.1 wavelength. Specimen length was measured with a micrometer which read directly to 0.0001 cm. The micrometer and specimen were thermostated on a large block of aluminum. The micrometer was checked against grade A-1 gauge blocks.

Specimen density was determined using the method of Archimedes. This was chosen as the means for obtaining the most accurate density values. This is important, as the elastic properties are calculated from the sound velocities; and, to minimize degrading the data computed from the sound velocities, the density must be known with equivalent accuracy. To obtain the desired accuracy, it is necessary to correct for all bouyancy effects and for surface tension forces on the suspending fiber. To minimize the latter effect, it is desirable to use a fiber which has a large

contact angle at the air-water interface, and as small a cross section as possible. Nylon fiber, 4 mil diamter, and a contact angle of 70°20' were used. A Mettler semi-micro balance, reproducible to 0.00003 gms, was employed in all the mass determinations. It should be noted that accurate bulk densities can be obtained in this manner only for impermeable specimens.

B. Pressure and Temperature Measurement

The 4 kbar pressure system is shown in Figure 1. A 60,000 psi S-C pump is the primary pressure generator. It delivers oil to one side of the mercury piston gas compressor. The mercury column functions as a frictionless piston and serves to separate the oil and gas sides of the system. Pressure is measured on a 0-75,000 psi Heise gauge, which is connected to a dead weight tester for calibration. The compressed gas is fed into the vessel which contains the specimen and holder. Leads through the cap of the vessel provide the means of applying the r-f signal. A copper-constantan thermocouple is brought through the cap of the vessel also. In this manner, the actual specimen temperature is monitored within the pressure vessel. A Leeds & Northrup K-3 potentiometer was used to measure thermocouple output.

For the low temperature runs, the vessel was placed in a cryostat containing crushed dry ice. For room

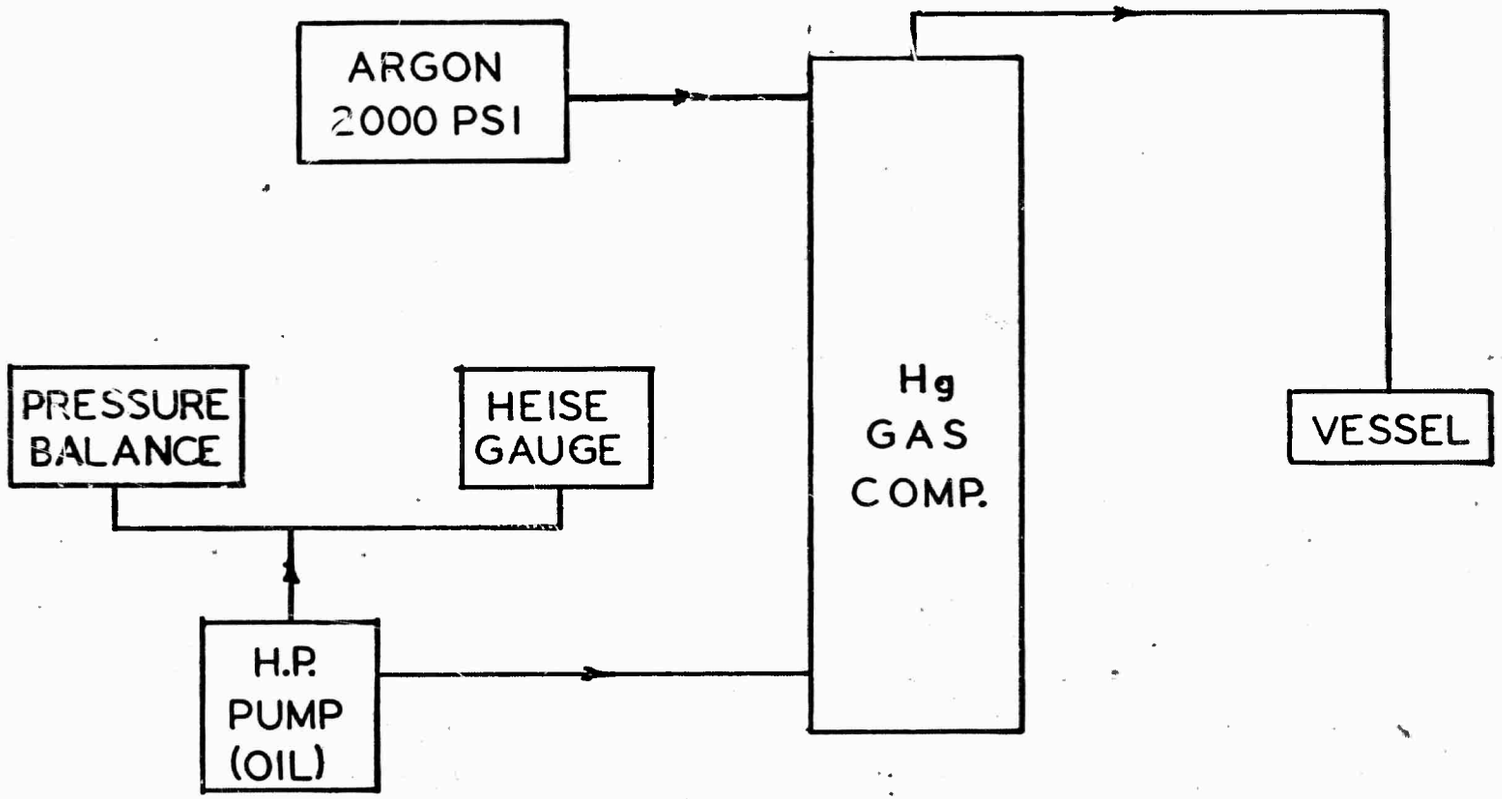

FIG 1: BLOCK DIAGRAM OF THE 4 KILOBAR PRESSURE SYSTEM

temperature runs, the vessel was circled with copper tubing through which water was circulated from a thermostated bath. Measurements at intermediate temperatures were obtained as the vessel was slowly cooled to the temperature of dry ice.

C. Velocity Measurements and Elastic Properties Determination

The techniques for measuring the sound velocity were ultrasonic interferometry. The methods of phase comparison and pulse superposition were both employed. The details of these methods are discussed in Appendix B. Both methods depend on interfering the radio frequency energy in a pulse applied to the specimen with the energy in the return echo. By taking advantage of the interference effects, measurements of transit time accurate to 0.001% are attainable, permitting velocity determinations accurately to 0.01%. The sensitivity of the method for detecting changes in transit time as small as 0.1 nanosecond make the methods ideal for determining velocity change as a function of pressure or temperature. In practice, one measures the initial velocity, v_o, at ambient conditions, and then measures the change in frequency, (time^{-1}), as a function of pressure or temperature. The velocity at the new condition is calculated from

$$v = v_o \left(\frac{f}{f_o}\right)\left(\frac{\ell}{\ell_o}\right) \qquad (1)$$

where f/f_o is the ratio of frequency at the new condition to the frequency at the initial (ambient) conditions and ℓ/ℓ_o is the length ratio for the two conditions in the direction of sound propagation. In temperature runs, the change in length is determined from thermal expansion data. For pressure runs, the ratio, ℓ/ℓ_o, is obtained by integrating the frequency dependence of the velocity modes with pressure (see Appendix B). In this manner the variation of the velocities with pressure or temperature are accurately determined. Because one measures the velocities directly and the density is determinable [$\rho = \rho_o(\ell_o/\ell)^3$], the adiabatic elastic properties are defined. Of particular interest are the shear modulus, G_S, bulk modulus, B_S, and Poisson's ratio, σ, which are given by

$$G_S = \rho v_S^2 \tag{2a}$$

$$B_S = \rho(v_p^2 - 4/3\ v_S^2) \tag{2b}$$

$$\sigma = 1/2\ \left\{1 - [(v_p/v_S)^2 - 1]^{-1}\right\} \tag{2c}$$

where v_S and v_p are the shear and compression velocities of an isotropic solid.

The variation of the moduli with pressure or temperature are given by

$$\left(\frac{\partial G_S}{\partial T}\right)_P = 20\rho v_S(\partial v_S/\partial T)_P - G_S\alpha_V \tag{3a}$$

$$\left(\frac{\partial G_S}{\partial P}\right)_T = 20\rho v_S \left(\frac{\partial v_S}{\partial P}\right)_T - 10\rho/B_S \tag{3b}$$

and

$$\left(\frac{\partial B_S}{\partial T}\right)_P = 20\rho \left[v_p \left(\frac{\partial v_p}{\partial T}\right)_P - \frac{4}{3} v_S \left(\frac{\partial v_S}{\partial T}\right)_P\right] - \alpha_v B_S \tag{4a}$$

$$\left.\begin{aligned}\left(\frac{\partial B_S}{\partial P}\right)_T = 20\rho \left[v_p \left(\frac{\partial v_p}{\partial P}\right)_T - \frac{4}{3} v_S \left(\frac{\partial v_S}{\partial P}\right)_T\right] \\ + 1 + \alpha_v \gamma T\end{aligned}\right\} \tag{4b}$$

In the above equations ρ is in gms/cm^3, α_v is the volume expansion, and γ is the Gruneisen constant given by

$$\gamma = \frac{\alpha_v B_S}{\rho C_p} \tag{5}$$

where C_p is the heat capacity at constant pressure.

To compare results of compressibility obtained from acoustic data with those obtained from compression measurements, one must take into account the adiabatic to isothermal correction. As $G_S = G_T$ (the T subscript is used to represent the isothermal condition), corrections are needed only for the bulk modulus. This may be obtained through the relations (see Appendix C for details):

$$B_T = B_S(1 + T\alpha_v\gamma) \tag{6}$$

The isothermal pressure derivative of the bulk modulus is given by

$$\left(\frac{\partial B_T}{\partial P}\right)_T = \left(\frac{\partial B_S}{\partial P}\right)_T + T\alpha_V\gamma\left(\frac{C_V}{C_p}\right)\left[\frac{-2}{\alpha_V B_T}\left(\frac{\partial B_T}{\partial T}\right)_P - 2\left(\frac{\partial B_S}{\partial T}\right)_P\right] + \left[T\alpha_V\gamma\left(\frac{C_V}{C_p}\right)\right]^2\left[\left(\frac{\partial B_S}{\partial P}\right)_T - \frac{1}{\alpha_V^2}\left(\frac{\partial \alpha_V}{\partial T}\right) - 1\right] \tag{7}$$

and the temperature derivative of the isothermal bulk modulus obtained from equation (6) is given below.

$$\left(\frac{\partial B_T}{\partial T}\right)_P = \left(\frac{\partial B_S}{\partial T}\right)_P \left(1 + T\alpha_V\gamma\right)^{-1} - \frac{B_S\gamma}{(1+T\alpha_V\gamma)^2}\left[\alpha_V + T\left(\frac{\partial \alpha_V}{\partial T}\right)_P\right] \tag{8}$$

D. Experimental Results

Velocity measurements were performed on the MgO and Al_2O_3 specimens as a function of pressure and of temperature, as described previously and in Appendix A. These measurements were performed under the following conditions: (1) isothermal pressure runs at ambient or near ambient temperature; (2) isobaric temperature runs down to -78.5°C

(the sublimation temperature of dry ice) at 1 atmosphere pressure; and (3) isothermal pressure runs at -78.5°C. The detailed results, which we submitted for publication,[6,7,8] are given in Appendix D. The pressure runs were to 4 kbars, except for MgO at -78.5°C.which was to 2 kbars. In Tables I and II the properties computed from these basic data are listed for magnesium oxide and aluminum oxide respectively.

The data indicates that the shear and longitudinal velocities of both materials are linear with pressure; and the bulk modulus is linear with pressure for both these materials. This is important because we are now able to use two methods[9] for calculating compression into the hundred kilobar region from this precise data which was measured at low temperatures.

The first method for deriving a compression curve depends upon the approximation that the isothermal bulk modulus is linear with pressure; i. e.,

$$B = -V_o\left(\frac{dP}{dV}\right) = B_o + C_o' P \qquad (9)$$

Expanding the volume isothermally by a Maclaurin's series to order P^4, we have

$$V(P) = V(0) + V'(0)P + \frac{1}{2}V''(0)P^2 + \frac{1}{6}V'''(0)P^3 + \frac{1}{24}V''''(0)P^4 \qquad (10)$$

TABLE I. Comparison of properties determined at -78.5°C and 34.6°C for MgO

PROPERTY	TEMPERATURE		UNITS
	-78.5°C	34.6°C	
Long. Velocity, v_P at P=0	9.8179	9.7662	km/sec
Shear Velocity, v_S at P=0	6.0138	5.9635	km/sec
$(\partial v_P/\partial P)_T$	7.57×10^{-3}	7.711×10^{-3}	km/sec/kbar
$(\partial v_S/\partial P)_T$	4.07×10^{-3}	4.351×10^{-3}	km/sec/kbar
$(\partial v_P/\partial T)_{P=0}$	4.3×10^{-4}	5.0×10^{-4}	km/sec/°C
$(\partial v_S/\partial T)_{P=0}$	3.6×10^{-4}	4.8×10^{-4}	km/sec/°C
Adiabatic Bulk Mod. B_S, P=0	1729.4	1717.0	kbars
Isothermal Bulk Mod. B_T, P=0	1717.1	1691.0	kbars
$(\partial B_S/\partial P)_T$	4.00	3.92	
$(\partial B_T/\partial P)_T$	4.02	3.94	
$(\partial B_S/\partial T)_{P=0}$	-0.11	-0.13	kbars/°C
$(\partial B_T/\partial T)_{P=0}$	-0.25	-0.29	kbars/°C
Gruneisen Constant	1.67	1.60	
Poisson's Ratio	0.200	0.203	
Density	3.5903	3.5800	gm/CC

TABLE II. Comparison of properties determined at -78.5°C and 25°C for Al_2O_3.

PROPERTY	TEMPERATURE -78.5°C	TEMPERATURE 25°C	UNITS
Long. Velocity, v_p at P=0	10.880	10.845	km/sec
Shear Velocity v_s at P=0	6.4028	6.3730	km/sec
$(\partial v_p/\partial P)_T$	5.075×10^{-3}	5.175×10^{-3}	km/sec/kbar
$(\partial v_s/\partial P)_T$	2.107×10^{-3}	2.207×10^{-3}	km/sec/kbar
$(\partial v_p/\partial T)_{P=0}$	-2.92×10^{-4}	-4.45×10^{-4}	km/sec/°C
$(\partial v_s/\partial T)_{P=0}$	-2.07×10^{-4}	-3.19×10^{-4}	km/sec/°C
Adiabatic Bulk Mod. B_S, P=0	2534.2	2520.6	kbars
Isothermal Bulk Mod. B_T, P=0	2526.8	2504.5	kbars
$(\partial B_S/\partial P)_T$	4.00	3.98	
$(\partial B_T/\partial P)_T$	4.01	3.99	
$(\partial B_S/\partial T)_p$	-0.118	-0.138	kbar/°C
$(\partial B_T/\partial T)_p$	-0.163	-0.207	kbar/°C
Gruneisen Constant	1.23	1.32	
Poisson's Ratio	0.2351	0.2363	
Density	3.9773	3.9720	gms/cm^3

where the primes denote derivatives with respect to pressure. Solving for the compression equation using (9) and the necessary operations on (2a), we have

$$\frac{V}{V_o} = 1 - \left(\frac{P}{B_o}\right) + m\left(\frac{P}{B_o}\right)^2 - n\left(\frac{P}{B_o}\right)^3 + q\left(\frac{P}{B_o}\right)^4 \qquad (11)$$

where

$$m = 1/2(1 + B_o') \qquad (12)$$

$$n = 1/6\,[1 + 3B_o' + 2(B_o')^2 - B_oB_o''] \qquad (13)$$

$$q = 1/24\,[11(B_o')^2 + 6B_o' + 6(B_o')^3 + 1 - 4B_oB_o'' - 6B_oB_o'B_o'' + B_o^2B_o'''] \qquad (14)$$

Equation (11) holds to a pressure given by

$$P^* = 3/2[B/(1 + 2B_o')] \qquad (15)$$

It turns out that P^* is 290 kbars for MgO and 419 kbars for Al_2O_3.

In (13) and (14) all terms involving B_o'' and B_o''' are ignored consistent with (9). This is an arbitrary assumption which can be refined by future theoretical and experimental work.

The second method for deriving a compression curve may be found by assuming that the instantaneous bulk modulus is

a linear function of pressure. That is, instead of (9), we have

$$B = -V\left(\frac{dP}{dV}\right) = b + aP \tag{15}$$

Murnaghan[10] defined and integrated (15) to find

$$P = \frac{b}{a}\left[\left(\frac{V_o}{V}\right)^a - 1\right] \tag{16}$$

Equation (16) is called the Murnaghan logarithmic equation. Murnaghan[10] found that the acoustic value of a is B_o'; and it appears obvious that $b = B_o$. Thus, acoustic data defines the parameters used in the Murnaghan logarithmic compression equation

$$\ln\left(\frac{V_o}{V}\right) = \left(\frac{1}{B_o'}\right)\ln\left[B_o'\left(\frac{P}{B_o}\right) + 1\right] \tag{17}$$

Using the isothermal values of the bulk modulus and its pressure derivative, we have, for MgO and Al_2O_3, the equations

$$\text{MgO:}\quad \left(\frac{V}{V_o}\right) = 1 - \left(\frac{P}{B_o}\right) + 2.475\left(\frac{P}{B_o}\right)^2 - 7.343\left(\frac{P}{B_o}\right)^3 + 23.59\left(\frac{P}{B_o}\right)^4$$

$$B_o = 1692 \text{ kbars} \tag{18a}$$

$$Al_2C_3: \quad \left(\frac{V}{V_o}\right) = 1 - \left(\frac{P}{B_o}\right) + 2.50 \left(\frac{P}{B_o}\right)^2 - 7.509 \left(\frac{P}{B_o}\right)^3 + 24.42 \left(\frac{P}{B_o}\right)^4$$

$$B_o = 2504 \text{ kbars} \tag{18b}$$

and

$$\text{MgO:} \quad \ell n \left(\frac{V_o}{V}\right) = 0.253 \ \ell n \left[3.94 \left(\frac{P}{B_o}\right) + 1\right] \tag{19a}$$

$$Al_2O_3: \quad \ell n \left(\frac{V_o}{V}\right) = 0.025 \ \ell n \left[3.99 \left(\frac{P}{B_o}\right) + 1\right] \tag{19b}$$

To test these equations, values of (V/V_o) were computed from equations (18) and (19). The results for MgO are compared with the compression data of Perez-Albuerne and Drickamer[11] in Table III. The result of the calculations for Al_2O_3 are compared with the compression data of Hart and Drickamer[12] and are shown in Table IV.

Another important result is the evaluation of the critical temperature gradient for MgO and Al_2O_3. The critical temperature gradient is that value of $(dT/dP)_v$ which when applied to the material just causes the sound velocity to be refracted with positive curvature. Thus, if the critical temperature gradient is exceeded, the appropriate sound velocity will decrease. From our measurement of the derivatives of sound velocity, we can form the derivative, at constant velocity (P or S)

TABLE III. Comparison of calculated with measured compression for MgO.[11]

Measured Compression		Predicted from 4 kbars Measurements			
		Murnaghan Log. Eq.		Polynomial Eq.	
P kbars	Meas. V/V_o	Calc. V/V_o	Error, in Percent	Calc. V/V_o	Error, in Percent
25	.987	.986	-0.10	.986	-0.10
50	.974	.972	-0.21	.972	-0.21
75	.963	.960	-0.31	.960	-0.31
100	.951	.948	-0.32	.948	-0.32
150	.930	.927	-0.32	.927	-0.32
200	.910	.908	-0.22	.909	-0.11
250	.893	.890	-0.34	.894	+0.11
300	.877	.874	-0.32	.882	+0.57
350	.862	.860	-0.23	.877	+1.74

TABLE IV. Comparison of calculated with measured compression for Al_2O_3.[12]

Measured Compression		Predicted from 4 kbars Measurements			
		Murnaghan Log. Eq.		Polynomial Eq.	
P kbars	Meas. V/V_o	Calc. V/V_o	Error, in Percent	Calc. V/V_o	Error, in Percent
63	0.98	.976	-0.4	.976	-0.4
128	0.96	.954	-0.6	.954	-0.6
192	0.94	.935	-0.5	.935	-0.5
256	0.92	.918	-0.2	.919	-0.1
288	0.91	.910	0	.911	+0.1
304	0.905	.906	+0.1	.907	+0.2

TABLE IV. Comparison of calculated with measured compression for Al_2O_3.[12]

Measured Compression		Predicted from 4 kbars Measurements			
		Murnaghan Log. Eq.		Polynomial Eq.	
P kbars	Meas. V/V_o	Calc. V/V_o	Error, in Percent	Calc. V/V_o	Error, in Percent
63	0.98	.976	-0.4	.976	-0.4
128	0.96	.954	-0.6	.954	-0.6
192	0.94	.935	-0.5	.935	-0.5
256	0.92	.918	-0.2	.919	-0.1
288	0.91	.910	0	.911	+0.1
304	0.905	.906	+0.1	.907	+0.2

$$\left(\frac{\partial T}{\partial P}\right)_V = - \frac{(\partial v/\partial P)_T}{(\partial v/\partial T)_P} \qquad (20)$$

which yields the temperature depth relation for these materials. For the slope of velocity with depth to change sign and, in particular, to become negative in the upper mantle, the earth must have properties such that

$$(dT/dP)_{EARTH} > (\partial T/\partial P)_{V\ (MATERIAL)} \qquad (21)$$

in the upper mantle, and reverses with depth.

From tables I and II we have the following velocity derivatives for MgO and Al_2O_3

	MgO		Al_2O_3		
	-78.5°C	34.6°C	-78.5°C	25°C	
$(\partial v_P/\partial P)_T$	7.57×10^{-3}	7.711×10^{-3}	5.075×10^{-3}	5.175×10^{-3}	*
$(\partial v_P/\partial T)_P$	-4.3×10^{-4}	-5.0×10^{-4}	-3.0×10^{-4}	-3.7×10^{-4}	**
$(\partial v_S/\partial T)_T$	4.07×10^{-3}	5.351×10^{-3}	2.107×10^{-3}	2.207×10^{-3}	*
$(\partial v_S/\partial T)_P$	-3.6×10^{-4}	-4.8×10^{-4}	-2.2×10^{-4}	-3.1×10^{-4}	**

* km/sec/kbar
** km/sec/°C

and from (20) and a value of 3.3 km/kbar for the pressure-depth relation in the upper mantle, we have the results (where Z is depth)

	MgO		Al_2O_3		
	-78.5°C	34.6°C	-78.5°C	25°C	
$(\partial T/\partial Z)_{v_P}$	5.33	4.67	5.12	4.23	°C/km
$(\partial T/\partial Z)_{v_S}$	3.42	2.75	2.90	2.15	°C/km

We estimate $\partial(\partial T/\partial Z)/\partial T$ to be -5.9×10^{-3}/km for constant v_p and v_s for MgO, and -8.6 (constant v_p) and -7.2×10^{-3} (constant v_s) for Al_2O_3. These values probably are less at higher temperatures, but do not alter the argument, as at higher temperatures the critical temperature gradient would be less than at 25°C.

Values for $(dT/dZ)_{EARTH}$ which have been deduced previously are 6.6°C/km,[13] 3.1°C/km,[14] and 7.46°C/km.[15] It is apparent that these two materials, which are constituents of the earth's crust, meet the condition necessary for a negative velocity slope. Figures 2A and 2B illustrate this condition. In figures 2A and 2B the temperature-pressure profiles for two geothermal models are superposed on a cross-plot of temperature versus pressure at constant velocity, derived from the data above. Figure 3 is the result showing how the sound velocities for P and S would vary with depth for MgO and Al_2O_3 if the temperature-pressure profile for the earth is imposed on either material. The relation between the material property and the geothermal gradient in

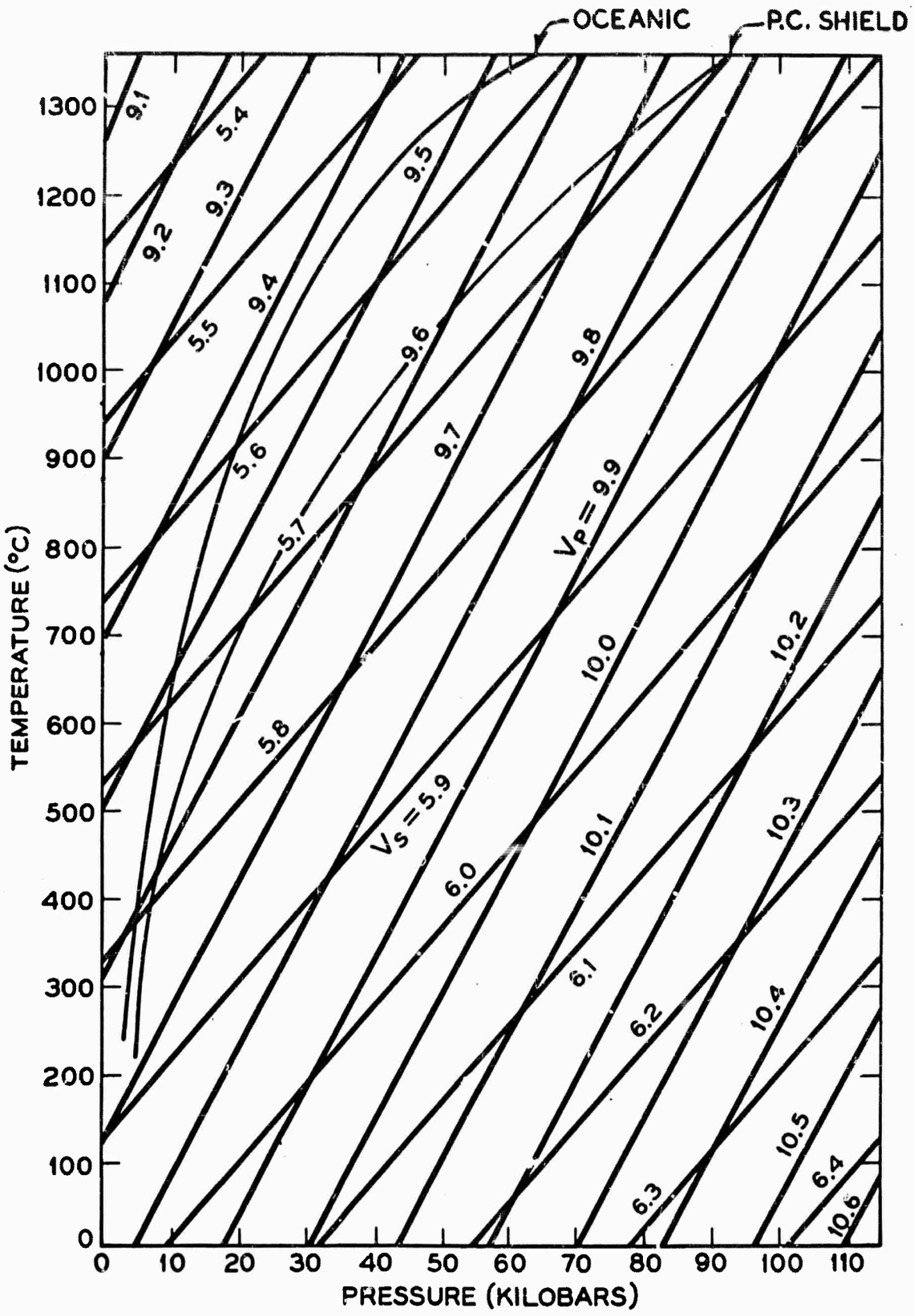

FIG 2A: T-P PLOT AT CONSTANT SOUND VELOCITY FOR MgO WITH GEOTHERMIC GRADIENTS SUPERPOSED

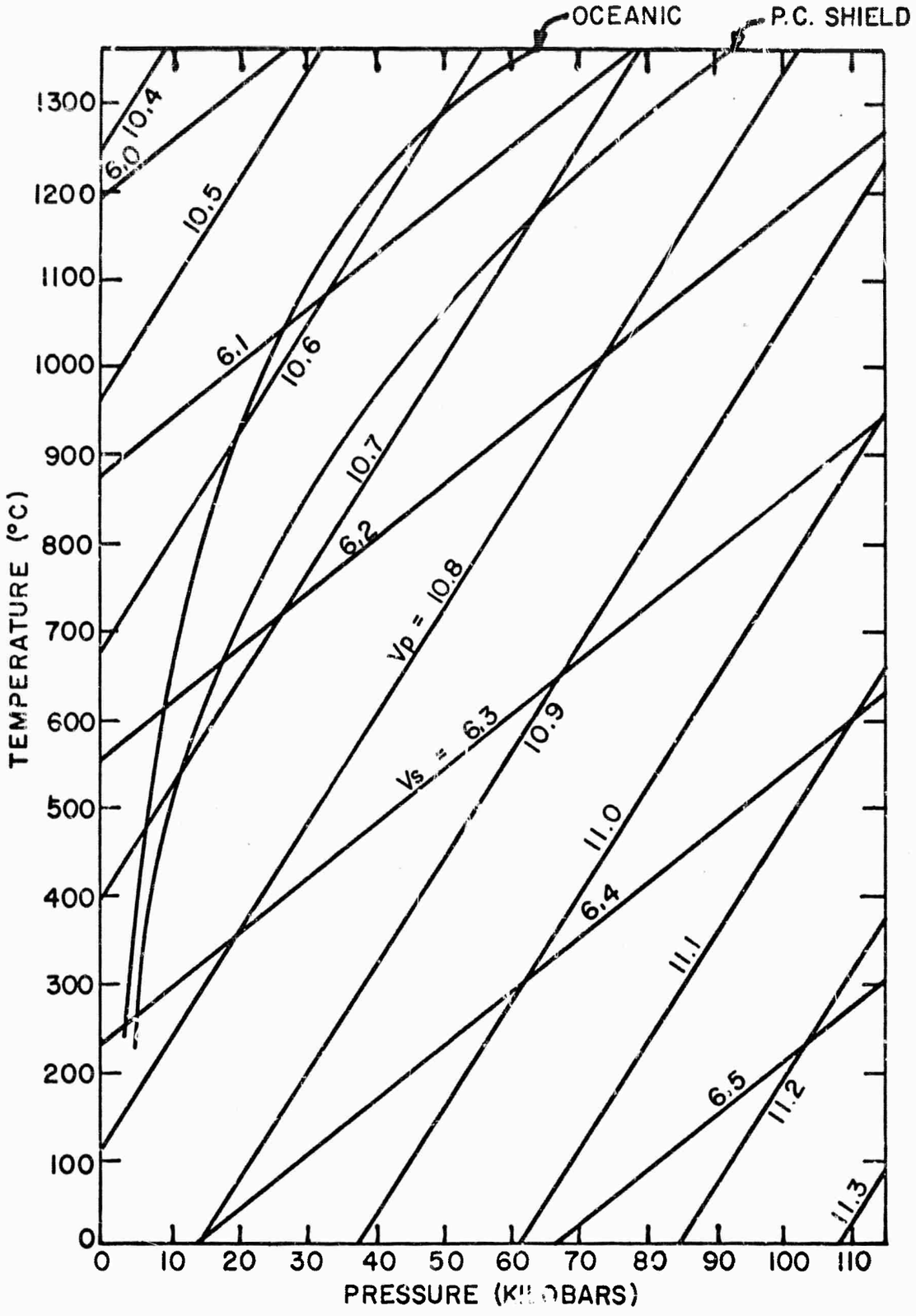

FIG 2B: T-P PLOT AT CONSTANT SOUND VELOCITY FOR Al_2O_3 WITH GEOTHERMIC GRADIENTS SUPERPOSED

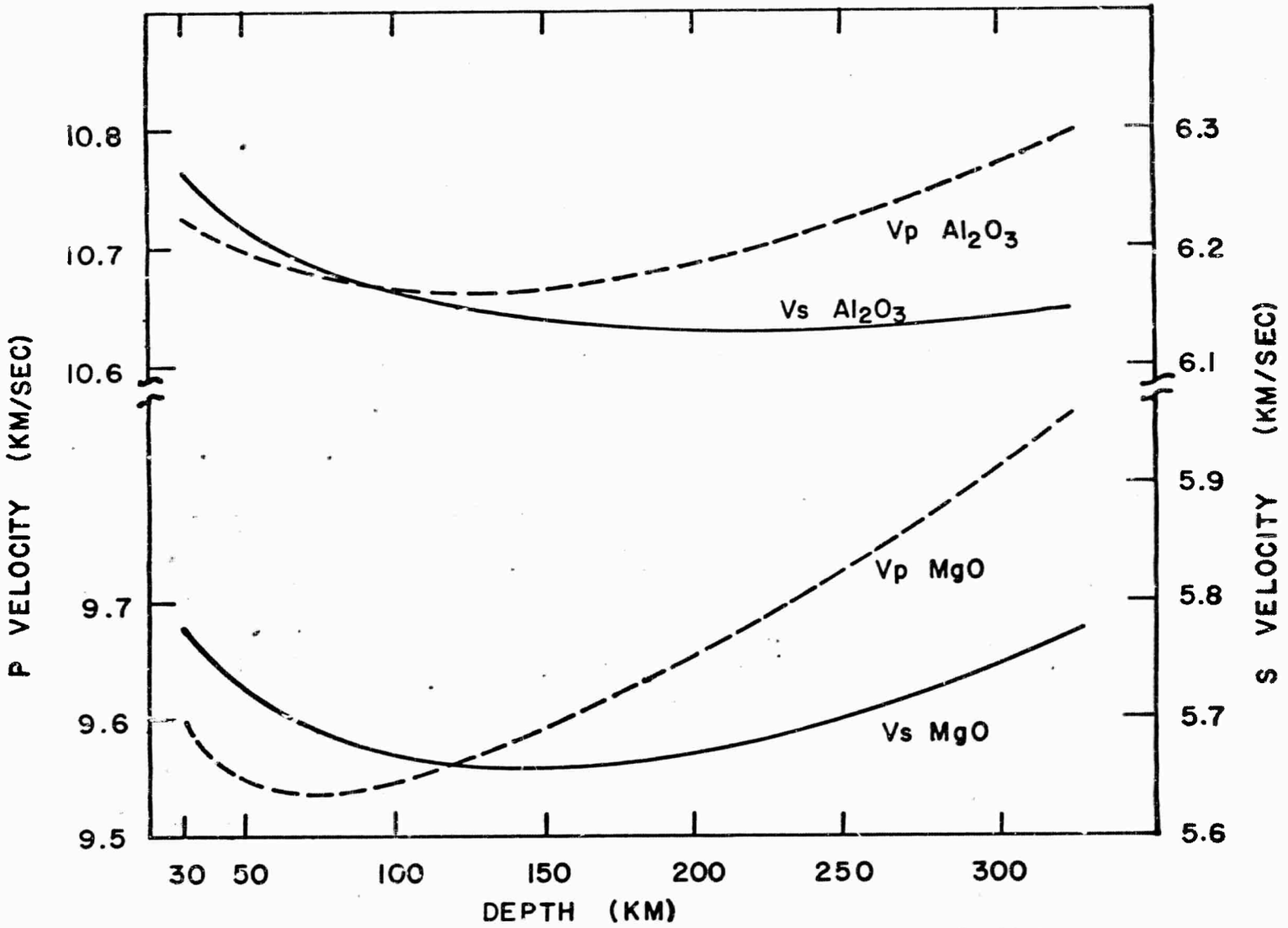

FIG. 3: VELOCITY-DEPTH PROFILES OBTAINED FOR MgO & Al_2O_3

producing a velocity minimum is made strikingly evident. It is apparent that for a given geothermal gradient, the material property of $(\partial T/\partial P)_V$ determines the depth of the velocity minimum. Thus a known variation in depth of the minimum velocity layer may be attributed to variation in the geothermal gradient, or material.

On the basis of the above, it would appear that

1. The observed velocity minimum in the mantle can exist as a consequence of the individual material property, and one need not assume, a priori, a need for a non-homogeneous mantle to explain this.

2. Variation of the depth at which the velocity minimum occurs may be attributed to a variation in the material property.

3. Variation of velocity at constant depth could be due to composition difference, but as lateral variation of the geothermal gradient could also produce this effect, it may be attributable to both factors.

4. As the critical velocity gradients for P are greater than for S, shallow P and pronounced S velocity minima result from the behavior of the materials.

IV. RECOMMENDATION FOR FUTURE WORK

The results of the present program have borne out the point of view, expressed in the proposal, that it is highly

profitable to perform experiments with precision enough to define the pressure and temperature derivatives of the velocity of mono-mineral compacts. Because of the complexity of the earth, it is important to be able to obtain sufficient data, so that the common denominators may be abstracted; and from these denominators obtain a broader, and yet more detailed understanding of the deep earth. We believe that it is important to extend these measurements to other minerals, either as polycrystalline compacts or, where these are not available, to single crystals. It is important, for example, to determine dB/dP for other minerals and see if it is near 4; and if d^2B/dP^2 is zero. Also of importance are the ways in which the derivatives of velocity differ from material to material, and the effects of these differences on velocities with depth. These considerations raise the following questions:

1. Are the derivatives of such numerical values that the velocities of different minerals tend to converge or diverge with increasing pressure and temperature?

2. Do all oxides and silicates have critical thermal gradients similar to MgO and Al_2O_3?

These are significant and important questions, which bear directly on an understanding of the mantle. It is desirable to employ materials which are thought representative of the mantle. However, this should not be an absolute

criteria for choosing specimens. As more information is gained about many materials, it will become possible to predict the behavior of any particular mineral.

ACKNOWLEDGEMENT

The skills of Mr. James Layfield for his contribution in design and construction of high pressure components and specimen assemblies and to Mr. Paul Mattaboni who kept the electronics in order and assisted in the measurements are gratefully acknowledged.

References

1. Birch, F., The velocity of compressional waves in rocks to 10 kilobars, Part 1, J. Geophys. Res., 65 [4], 1083-1101, 1960.
2. Birch, F., The velocity of compressional waves in rocks to 10 kilobars, Park 2, J. Geophys. Res., 66 [7], 2199-2223, 1961.
3. Simmons, G., Velocity of compressional waves in various minerals at pressures to 10 Kbars, J. Geophys. Res., 69 [6], 1117-1121, 1964.
4. Simmons, G., Velocity of shear waves in rocks to 10 kilobars, J. Geophys. Res., 69 [6], 1123-1130, 1964.
5. Brace, W. F., Some new measurements of linear compressibility of rocks, J. Geophys. Res., 70 [2], 391-398, 1965.
6. Anderson, O. L., and E. Schreiber, The pressure derivatives of the sound velocities of polycrystalline magnesia, J. Geophys. Res., 70[20], 5241-5248, 1965.
7. Schreiber, E., and O. L. Anderson, The pressure derivatives of the sound velocities of polycrystalline alumina, J. Am. Ceram. Soc., in press.
8. Schreiber, E., and O. L. Anderson, The temperature derivatives of the velocities of polycrystalline magnesia, submitted for publication.
9. Anderson, O. L., Two methods for estimating compression and sound velocity at very high pressures, Proc. Nat'l. Acad. Sci., 54 [3], 667-673, 1965.

10. Murnaghan, F. D., The foundations of the theory of elasticity, Proc. Symp. Appl. Math., 1, 167, 1949.

11. Perez-Albuerne, E. A., and H. G. Drickamer, Effect of high pressure in the compressibility of 7 substances having the NaCl structure, J. Chem. Phys., in press.

12. Hart, H. V., and H. G. Drickamer, Effect of high pressure on lattice parameters of Al_2O_3, J. Chem. Phys., in press.

13. Birch, F., Elasticity and constitution of the earth's interior, J. Geophys. Res., 70[2], 391-398, 1952.

14. Valle, P. E., Ann. Geofiz Rome, 9, 371-377, 1956.

15. McDonald, G. J. F., and N. F. Ness, A study of the free oscillations of the earth, J. Geophys. Res., 66[6], 1865-1911, 1961.

APPENDIX A

ABSTRACTS OF PAPERS

The following abstracts are from the manuscipts which have resulted from our effort in the fullfillment of our contract.

1. "Conditions for a density minimum in the upper mantle", O. L. Anderson, J. Geophys. Res., 70 [6], 1457-1461, 1965.

Abstract. A number of recent articles have indicated that there is a density minimum in the upper mantle. An example is the article by Clark and Ringwood, where the density is based upon petrology. In this paper, the conditions for a density minimum are established using the Mie-Guneisen equation of state. It is shown that for a homogeneous mantle with a positive value of thermal expansivity, the sign of the density gradient is the same as the sign of the S velocity gradient, that is, $d(\ln v_S)/d(\ln\rho)>0$. The conditions for a density minimum in a nonhomogeneous mantle are also discussed.

2. "The relation between refractive index and density of minerals related to the earth's mantle", O. L. Anderson and E. Schreiber, J. Geophys. Res., 70 [6], 1463-1471, 1965.

Abstract. It is known that the density of many minerals is related to the (average) index of refraction

by a linear law called the Gladstone-Dale law. It is shown that this law is generally applicable only to minerals whose anion is oxygen and whose mean molecular weight is close to 21. Another relationship, called Drude's law, which is deduced from classical dielectric theory, fits the data just as well as the empirical linear law. The correlation between density and index includes the minerals arising from various combinations of SiO_2, MgO, Al_2O_3, Na_2O, and K_2O. An implication is that density controls certain physical properties of oxides, independently of composition or crystal class. This is analogous to the rule found by Birch which relates sound velocity to density and holds for the same groups of minerals.

3. "Lattice dynamics in geophysics", O. L. Anderson, Trans. N. Y. Acad. Sci., Ser. II, 27 [3], 298-308, 1965.

Abstract. An arbitrary but useful way to classify solid physical properties is into the classes of lattice properties or defect properties. In lattice dynamics, the word lattice indicates lattice properties and the word dynamics indicates the importance of thermal vibrations of atoms to those properties. Examples of lattice dynamics properties are: infrared reflection, specific heat, thermal

expansivity, sound velocity, melting temperature, and thermal diffuse x-ray scattering. These properties are defined in terms of the set of normal vibrational modes, calculated from a model composed of discrete masses connected by springs in a large array. This information is contained in a fundamental diagram, associated with the particular model, called the frequency vs. wave number diagram. (ν-k).

The importance of lattice dynamics, as far as geophysics is concerned, is that all lattice properties are functions of the atomic mass, spacing, and spring constant of the model. Therefore, any lattice property is derivable from other lattice properties. In particular it is possible to estimate several important lattice properties from the sound velocity and density. To geophysicists the field of lattice dynamics provides a set of principles by which thermal, optical, and thermodynamic properties can be estimated from seismic data.

4. "The Bulk Modulus Volume Relationship for Oxide Compounds and Related Geophysical Problems", O. L. Anderson and J. Nafe, J. Geophys. Res., 70 [16], 3951-3963, 1965

Abstract. The relationship between the sound velocity and density in various oxide compounds at atmospheric pressure is relevant to problems of the earth's interior. Here, data on elastic constants of various compounds are collected and analyzed. It is shown that the bulk modulus-volume per ion pair relationship for oxide compounds differs in a remarkable degree from that found for alkali halides, fluorides, selenides, sulfides, and covalent compounds.

It is shown that a change of volume has the same effect on the bulk modulus of oxide compounds, whether the volume change is produced by pressure, compositional variation, phase changes, temperature, or porosity. It thus appears that volume is the primary variable affecting the elastic moduli of oxide compounds, and all other variables affect the moduli only insofar as they affect the volume itself.

5. "An approximate method of estimating shear velocity from specific heat", O. L. Anderson, J. G. R., 70 [18], 4726-4728, 1965.

Abstract. The shear velocity may be estimated from low temperature specific heats because at low temperatures the contribution to the specific heat is due to acoustic vibrations. The low temperature

specific heat is characterized by the "Debye" temperature and the shear velocity may be estimated from the Debye temperature. The source of discrepancies and the general implications are discussed.

6. "The pressure derivatives of the sound velocities of polycrystalline magnesia", O. L. Anderson and E. Schreiber, J. G. R., 70: [20], 5241-5248, 1965.

Abstract. A polycrystalline sample of MgO was obtained of gem quality. The sound velocities and the pressure derivatives of the sound velocities were measured by the "phase comparison"technique. The pressure derivatives found from experiments up to 4 kilobars are:

$$\frac{dv_s}{dp} = 4.351 \times 10^{-3} \text{ km/sec/kbar}$$

$$\frac{dv_p}{dp} = 7.711 \times 10^{-3} \text{ km/sec/kbar}$$

Arguments are presented which indicate that these pressure derivatives hold up to at least 100 kilobars.

These values yield a vanishingly small value of the pressure derivative of Poisson's ratio.

The Gruneisen constants of the shear and longitudinal modes are calculated, from which the

acoustic Gruneisen constant is estimated to be 1.60. This agrees very well with the Gruneisen constant obtained from thermal properties.

7. "Two methods for estimating compression and sound velocity at very high pressures", O. L. Anderson, Proc. Nat. Acad. Sci., 54 [3], 667-673, 1965.

Abstract. Precision sound velocity measurements at relatively low pressure (less than 10 kilobars) can be used to estimate sound velocity and volume compression at very high pressures. If the parameters of a continuous analytic function are sufficiently accurately determined at low values of the independent variable, the function may be evaluated at high values of the independent variable. Consequently, only materials undergoing compression without phase change are treated.

What is new is the presentation of two functions suitable for representing volume dependence upon pressure (compression curves) and the evaluation of the parameters in these functions from acoustic data taken at low pressures but with high precision. The parameters are the bulk modulus and its higher derivatives.

8. "The pressure derivatives of the sound velocity of polycrystalline alumina", E. Schreiber and O. L. Anderson, J. Am. Ceram. Soc., in press.

Abstract. The sound velocities and the pressure derivatives of the sound velocities were measured on a small sample of alumina (Lucalox) by the method of "pulse superposition". The pressure derivatives found from experiments up to 4 kilobars at 25°C are:

$$\frac{dv_s}{dP} = 2.207 \times 10^{-3} \text{ km/sec/kbar} \quad \text{(Shear Wave)}$$

$$\frac{dv_p}{dP} = 5.175 \times 10^{-3} \text{ km/sec/kbar} \quad \text{(Long. Wave)}$$

These values lead to the variation of Poisson's ratio with pressure of $d\sigma/dP = 1.02 \times 10^{-4}$/kilobar; and to the variation of (isothermal) bulk modulus with pressure of $dB_T/dP = 3.99$.

Using the above values the computed compression is determined up to 400 kilobars, and compares well with shock wave measurements. Consequently, the measured pressure derivatives may hold up to several hundred kilobars.

9. "Seismic parameter ϕ: Computation at very high pressure from laboratory data:, O. L. Anderson, Bull. Seism. Soc. Am., in press.

Abstract. By using the accuracy inherent in ultrasonic velocity measurements taken at pressures less

than 10 kb, the seismic parameter $\phi = v_p^2 - (4/3)\, v_s^2$ can be computed at very high pressures. The equation used requires the assumption that the second derivative with respect to pressure of the bulk modulus be negligible at all pressures considered. This assumption is checked by computing the compression (V/V_o) in the pressure range by equations of state using the assumption, and comparing the ressulting values with measured compression. Illustrations are given for MgO and Al_2O_3.

10. "Temperature dependence of the velocity derivatives of periclase", E. Schreiber and O. L. Anderson, submitted for publication.

Abstract. The temperature dependence of the sound velocity in polycrystalline MgO has been determined from +80 to -80°C and to 2 kbars at -78.5°C. These results are compared to previous measurements to 4 kbars at 34.6°C. From these measurements the critical temperature gradient $(\partial T/\partial P)_v$ for MgO was determined, and these values applied to the earth. Because $(\partial T/\partial P)_v$ was found to be greater for P waves than for S waves in MgO, and both are small compared to $(\partial T/\partial P)_v$ for the earth, it is possible to explain the existence of a low-velocity layer in a homogeneous earth.

APPENDIX B

MEASUREMENT OF SOUND VELOCITY BY MEANS OF ULTRASONIC INTERFEROMETRY

A. Phase Comparison

The technique involves many of the optical principles of multiple-beam interferometry. The ultrasonic technique, called "phase comparison" method, was originated by McSkimin[1] and is described below.

Figure 1A illustrates the electronic arrangement. A stable, variable frequency oscillator is employed as the RF carrier generator. This frequency is accurately measured by the frequency counter. The output of this oscillator is fed to the gated harmonic generator. The purpose of this component is to produce series of gated RF pulses at the desired frequency (in this case, 60 mc/sec). The frequency and width of these gated pulses are controlled by the General Radio 1217-B unit pulse generator. The output of the harmonic generator is applied directly to a quartz transducer (x or y cut for longitudinal or shear modes) which serves as a transmitter of the generated pulse and receiver of the echoes in the time slot between the generated pulses. The beat frequency oscillator is used for heterodyning to produce a 20 mc I.F. thus permitting the use of a single high gain I.F. amplifier. The output is also tied to an attenuator and then

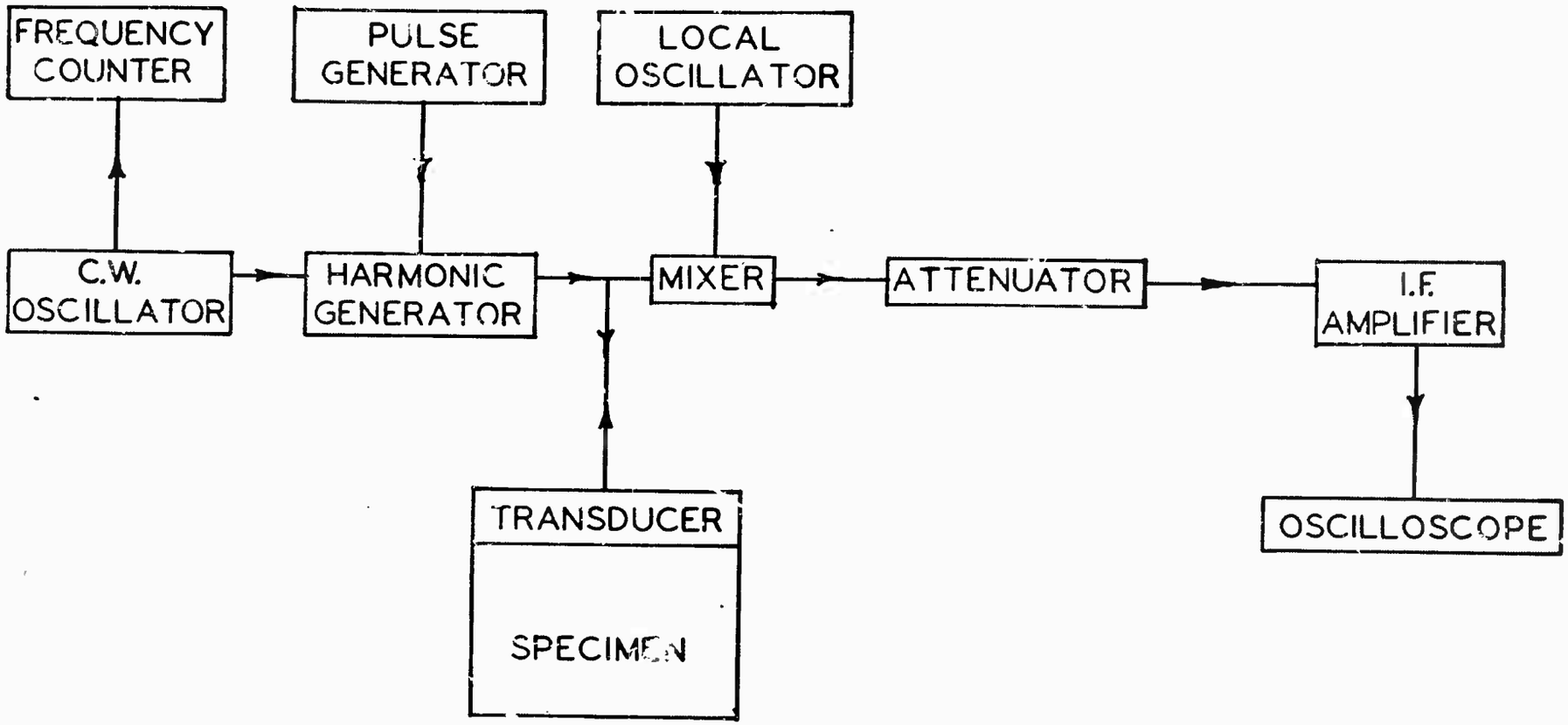

FIG 1A: ULTRASONIC INTERFEROMETER FOR PHASE COMPARISON

to the high gain I.F. amplifier. The output of this amplifier is displayed on a Tektronix 535A oscilloscope.

To measure the absolute velocity at ambient conditions a buffer rod of either quartz or vitreous silica is employed. A quartz transducer is bonded to one end of the buffer rod and performs as the driver. The sample is bonded to the other end of the rod with a suitable material (Dow-Corning resin blend V-9 for example). Part of the energy transmitted by the transducer is reflected at the opposite end of the buffer rod, and part is coupled into the specimen, via the bond, to be reflected back from the free end of the specimen. The output seen on the oscilloscope consists of the pulse applied to the transducer from the harmonic generator, the return echoes from the end of the buffer rod; and between the buffer rod echoes, the specimen echoes. The energy coupled from the buffer rod is now the applied pulse to the specimen. By broadening the pulse width so that the energy returning from the specimen echoes is overlapped by the applied pulse from the buffer rod, the 60 mc carrier is made to phase interfere. It is in this manner that the accuracy is obtained. A minima will be obtained when the RF frequency is such that specimen length is an integral number of wave lengths. From the condition for interference, the velocity is given by[1]

$$v = \frac{2\,\ell\,f}{n + \theta/360} \tag{1}$$

where v is the velocity in the specimen, ℓ is the specimen length, f the frequency, n the number of wave lengths in the specimen, and θ a small correction for phase shift introduced in the seal. The latter may be evaluated from the known acoustic impedances of the buffer rod, seal, and specimen as described by McSkimin[1]. When this correction is applied, velocity can be determined to an accuracy of at least one part in 10,000. The order n is determined by measuring a sequence of frequencies at which 'resonance' occurs and by using the following

$$n = \frac{f_n}{\Delta f} \tag{2}$$

where f_n is the resonant frequency for a particular n, and Δf the difference in f_n and $f_{(n+1)}$.

To measure the velocity with pressure or temperature, the transducer is bonded directly to the specimen and the specimen echoes are overlapped. The change in frequency at constant n is determined. The velocity at any pressure or temperature may be calculated from

$$v = v_o(f_n/f_{n_o})(\ell/\ell_o) \tag{3}$$

where the o subscripts refer to initial conditions. The ratio ℓ/ℓ_o may be obtained from expansivity data for temperature runs. The situation is slightly more involved for pressure runs. Cook[2] has shown that the value of the ratio ℓ/ℓ_o may be determined from the relation

$$\frac{\ell_o}{\ell} = 1 + \frac{1 + \Delta}{\rho_o} \int_o^P \frac{dP}{4A - 3B} \qquad (4)$$

where A is given by $(v_o f_n / f_{n_o})^2$ for longitudinal waves and B by the value $(v_o f_n / f_{n_o})^2$ for shear waves. The initial density is ρ_o and Δ is given by

$$\frac{9 \beta^2 T}{C_p \rho}$$

where C_p is the heat capacity, β is the coefficient of linear expansion, B_s is the adiabatic bulk modulus, and T is the absolute temperature. The atmospheric pressure values of the parameters are used in determining Δ, which leads to errors no more than about 0.01%, and the value of ℓ_o/ℓ is found as a function of pressure. In this manner the change of path length with pressure is accurately accounted for.

B. Pulse Superposition

Pulse superposition differs from phase comparison in that the frequency of the applied pulses is crucial to the measurement rather than the frequency of the carrier. This technique is also due to McSkimin.[3] It has the operating advantage of greater energy in the return echoes. Figure 1B is the block diagram of the electronic arrangement for pulse superposition (P.S.P.). The critical component is the pulsed oscillator.* The C.W. oscillator is of variable frequency design, with a range of 8 to 130 mc/sec permitting the use of a wide range of transducers. The C.W. oscillator is pulsed by the pulse repetition oscillator at a pulse repetition frequency (P.R.F.) of 1 mc or less. The output of the Uni-Pulse consists of a sequence of R.F. pulses which drive the X or Y cut transducers. The returning specimen echoes are received by the same transducer. The signal is fed to a mixer stage, a calibrated attenuator, and a high gain I.F. amplifier-detector. The detected signal is applied to a Tektronix 535A oscilloscope, where the envelopes of the pulses are displayed. The P.R.F. is accurately determined to six significant figures with the frequency counter. This method requires a very stable P.R.F., at least 1 part in 10^7.

*Uni-Pulse, mftrd by the W.M.A. Anderson Co., Pleasant Valley, Conn.

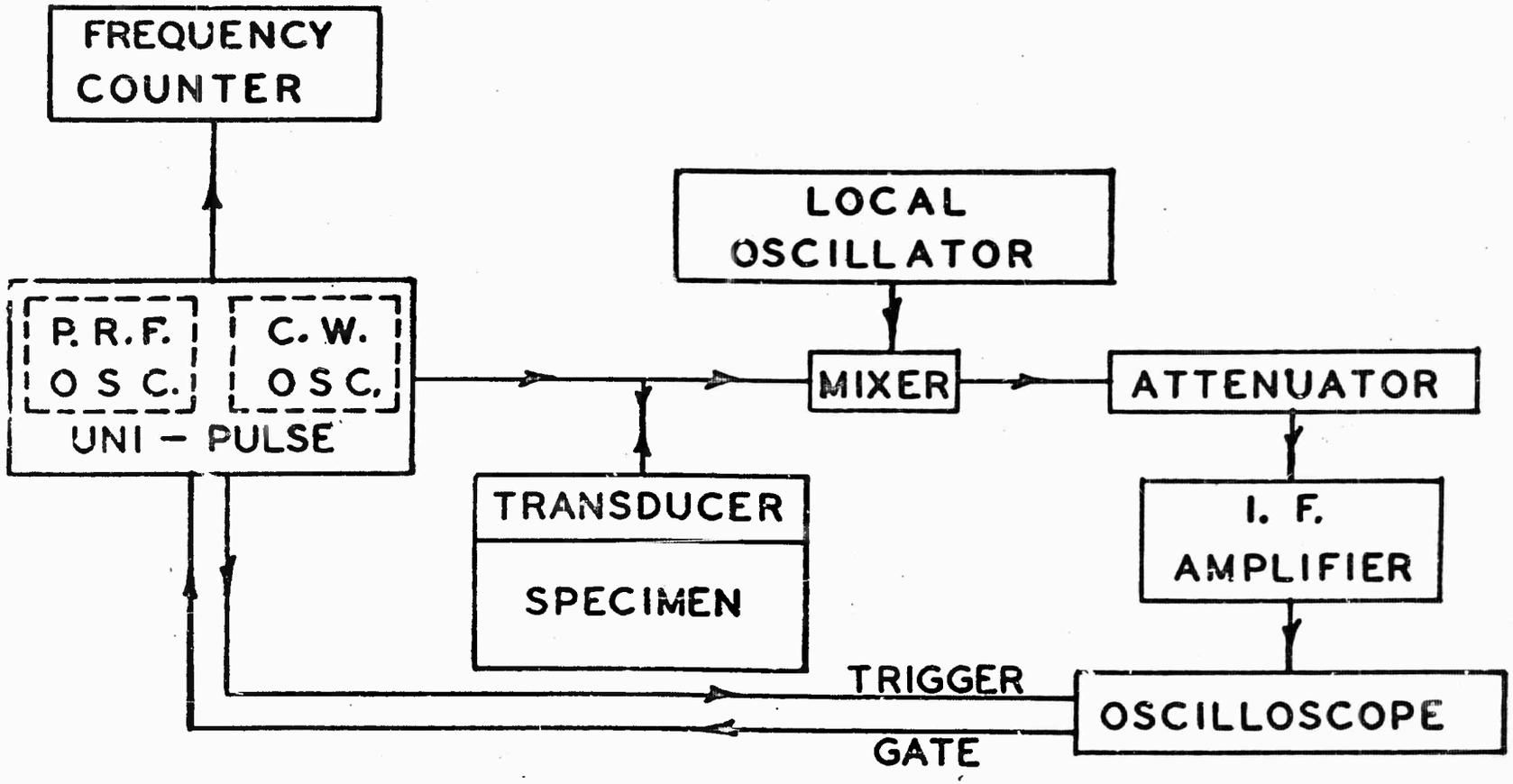

FIG 1B ULTRASONIC INTERFEROMETER FOR PULSE SUPERPOSITION

In principle, the P.R.F. is adjusted so that its period is equal to some integral sub-multiple of the delay time in the specimen. That is, the time delay between applied pulses (period of P.R.F.) is exactly equal to an integral number of round trips in the specimen. When this condition is achieved, the applied pulses are <u>superposed</u> upon the specimen echoes. If the integer is one, every specimen echo will have an applied pulse superposed upon it. If the integer is two, the applied pulses will be superposed upon every other echo, and so on. It is preferable to operate with this integer equal to unity, for then the greatest amount of energy is being impressed upon the specimen. At this condition, only the applied pulses are visible on the oscilloscope display. To observe the specimen echoes, a "window" is produced in the sequence of applied pulses by gating the pulsed oscillator. This is accomplished by applying a gating voltage from the oscilloscope to the Uni-Pulse. One now views the echoes and critically adjusts the P.R.F. to maximize their amplitudes. When critically adjusted, the applied pulse is superposed upon the echo, and the C.W. in the pulse is phase adding with the C.W. in the echo. The relation between the measured time delay (reciprocal of the P.R.F.) and the actual time delay in the specimen is given by[3]

$$\tau = p\delta - \frac{p\zeta}{360f} + \frac{n}{f} \qquad (5)$$

In (1) τ is the measured period of the P.R.F., at the interference condition, δ is the true time delay in the specimen, p is the integer discussed above, ζ is the phase shift introduced by the seal (transducer to specimen bond), f is the frequency of the C.W. oscillator, and n is an integer asscciated with the phasing between the C.W. within the applied pulse and within the return echo. To understand the meaning of n, consider Figure 2.

A constructive interference will occur every time a C.W. cycle in the pulse is exactly in phase with a C.W. cycle in the echo. A series of maxima may therefore be observed as the P.R.F. is varied. These maxima will be separated by differences in the P.R.F. corresponding to the period of the C.W. frequency. The maxima will be observed for each integral n for $n \leq 0 \leq n$. It is possible to determine the P.R.F. for which $n = 0$, as described by McSkimin.[3] Choosing the conditions $p = 1$ and $n = 0$, the true time delay in the specimen (time per round trip) is given by

$$\delta = \tau + \zeta/360f \qquad (6)$$

Generally, ζ is less than 1° for a properly prepared seal, and the C.W. carrier is of the order of 10^7 cycles/sec. The correction is of the order of 10^{-10} or less, so that even for precise measurements this correction may frequently

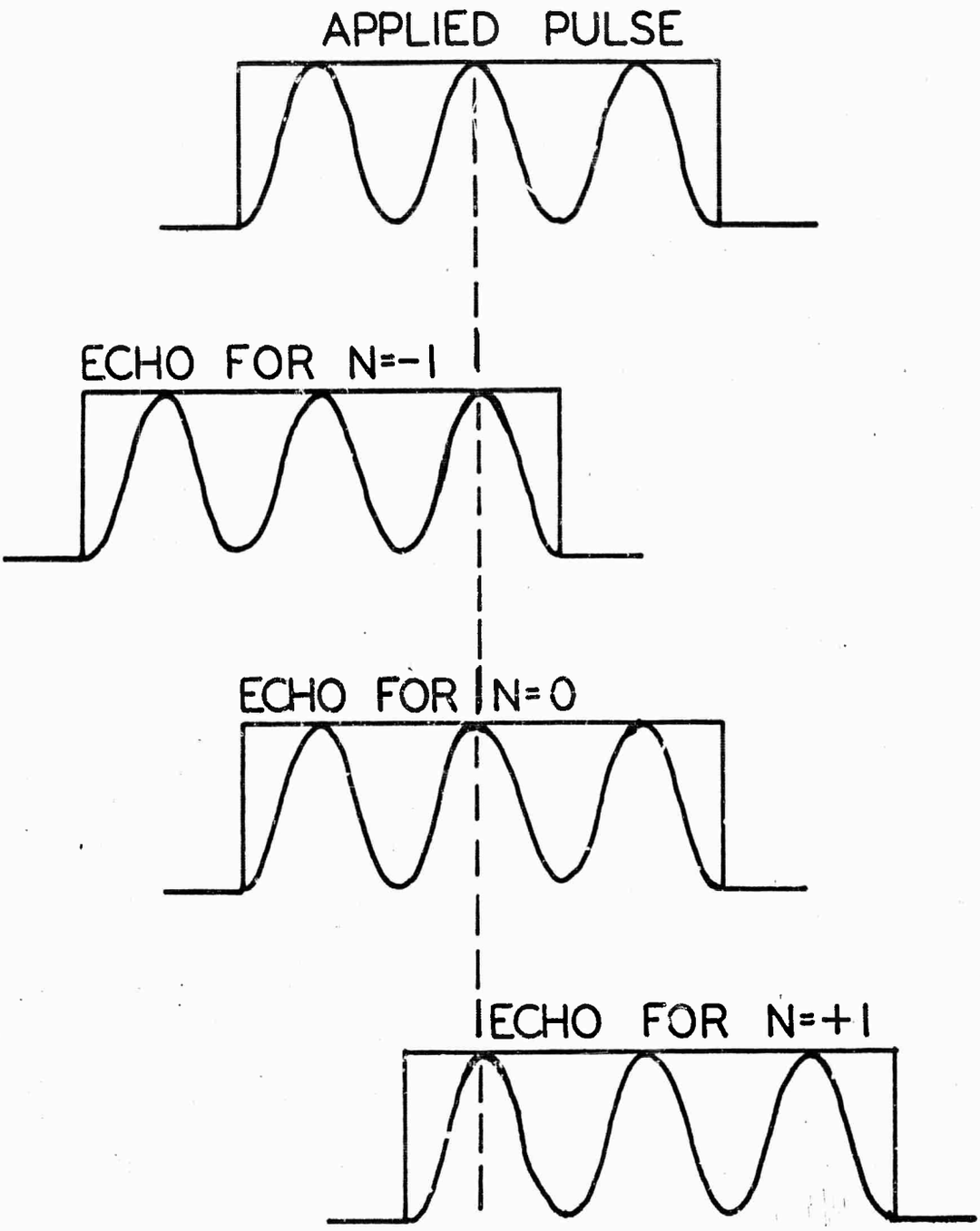

FIG 2: ILLUSTRATING THE MEANING OF THE INTEGER N

be ignored. The simple manner of dealing with these sources of systematic errors is a major advantage of pulse superposition.

A further advantage arises from the fact, that for C.W. frequencies near the transducer resonance frequency, the value of ζ is sensitive to changes of temperature and pressure.

The velocity of sound in the specimen is readily obtained once the specimen length ℓ is known. The velocity is given by

$$v = \frac{2\ell}{\delta} \tag{7}$$

As δ is generally known to 5-6 significant figures, the greatest limitation on the accuracy of v is the measurement of the specimen length in the direction of sound propagation.

The measurement of the velocity with pressure or temperature is the same as for phase comparison. The P.R.F. (at constant n) is measured and the ratio of f/f_o (δ_o/δ) used in (3) in place of f_n/f_{n_o}. The length ratio is also determined in the same manner as for phase comparison.

REFERENCES

1. McSkimin, H. J., Ultrasonic measurement techniques applicable to small solid specimens, J. Acous. Soc. Amer., 22, 413-421, 1950.

2. Cook, R. K., Variation of elastic constants and static strains with hydrostatic pressure; a method for calculation from ultrasonic measurements., J. Acous. Soc. Amer., 29[4], 445-449, 1957.

3. McSkimin, H. J., Pulse superposition method for measuring ultrasonic wave velocities in solids, J. Acous. Soc. Amer., 33, 12-16, 1961.

APPENDIX C

ADIABATIC TO ISOTHERMAL CORRECTIONS TO THE SECOND ORDER

The results of acoustic experiments yields the adiabatic elastic constants. It is desirable for numerous reasons to convert from adiabatic to isothermal conditions. In order to preserve the inherent accuracy of the acoutis measurements, an exact treatment is desirable. Overton[1] developed equations for cubic crystals. Below these are presented, modified, for the isotropic case.

The adiabatic-isothermal corrections are

$$C_p - C_v = TV\alpha^2/\chi_T \tag{1}$$

$$\chi_T - \chi_s = TV\alpha^2/C_p \tag{2}$$

$$G_s = G_T \tag{3}$$

where α is the volume coefficient of thermal expansion, C_v and C_p represent specific heats, V represents specific volume, χ represents compressibility, G represents shear modulus, and the subscripts s and T indicate adiabatic and isothermal conditions.

We have further that

$$\frac{B_S}{B_T} = \frac{C_p}{C_v} = \frac{\chi_T}{\chi_S}$$

where B represents bulk modulus.

The Gruneisen ratio is given by

$$\gamma = \frac{\alpha V B_T}{C_v} = \frac{\alpha V}{C_v \chi_T} \tag{4}$$

so that (1) and (2) also have the forms

$$C_p = C_v(1 + T\alpha\gamma) \tag{5}$$

$$\chi_T = \chi_S(1 + T\alpha\gamma) \tag{6}$$

Differentiating (2) we have,

$$\left(\frac{\partial \chi_T}{\partial P}\right)_T - \left(\frac{\partial \chi_S}{\partial P}\right)_T = \frac{TV\alpha^2}{C_p}\left[-\chi_T + \frac{2}{\alpha}\left(\frac{\partial \alpha}{\partial P}\right)_T - \frac{1}{C_P}\left(\frac{\partial C_P}{\partial P}\right)_T\right] \tag{7}$$

We now change the terms on the right side of (7) to measurable quantities. Using the identity,

$$\left(\frac{\partial C_P}{\partial P}\right)_T = -T\left(\frac{\partial^2 V}{\partial T^2}\right)_P = -TV\left(\frac{\partial \alpha}{\partial T}\right)_P$$

and

$$\left(\frac{\partial \alpha}{\partial T}\right)_P = -\frac{1}{V^2}\left(\frac{\partial V}{\partial T}\right)_P^2 + \frac{1}{V}\left(\frac{\partial^2 V}{\partial T^2}\right)_P$$

we have

$$\left(\frac{\partial C_P}{\partial P}\right)_T = -TV\left[\alpha^2 + \left(\frac{\partial \alpha}{\partial T}\right)_P\right] \tag{8}$$

Similarly

$$\left(\frac{\partial \alpha}{\partial P}\right)_T = -\left(\frac{\partial \chi_T}{\partial T}\right)_P \tag{9}$$

Equation (7) becomes

$$\left(\frac{\partial \chi_T}{\partial P}\right)_T - \left(\frac{\partial \chi_S}{\partial P}\right)_T = T\alpha\gamma\left(\frac{C_p}{C_v}\right)$$

$$\left\{-\chi_T^2 - \frac{2\chi_T}{\alpha}\left(\frac{\partial \chi_T}{\partial T}\right)_P + \frac{TV}{C_p}\left[\alpha^2 + \left(\frac{\partial \alpha}{\partial T}\right)_P\right]\right\} \tag{10}$$

The equivalent of (10) in terms of bulk modulus is, after some reduction,

$$\left(\frac{\partial B_T}{\partial P}\right)_T = \left(\frac{\partial B_S}{\partial P}\right)_T$$

$$+ T\alpha\gamma\left(\frac{C_v}{C_p}\right)\left[-\frac{2}{\alpha B_T}\left(\frac{\partial B_T}{\partial T}\right)_P - 2\left(\frac{\partial B_S}{\partial P}\right)_T\right]$$

$$+\left[T\alpha\gamma\left(\frac{C_v}{C_p}\right)\right]^2\left[\left(\frac{\partial B_S}{\partial P}\right)_T - 1 - \frac{1}{\alpha^2}\left(\frac{\partial \alpha}{\partial T}\right)_P\right] \tag{11}$$

The second term of (11) is small and positive and the third term is even smaller and ordinarily negative. The product $T\alpha\gamma$ is usually small, of the order of 1 or 2% at ordinary temperatures.

The terms used in obtaining the conversion for the adiabatic to isothermal conditions for the pressure variation of the bulk modulus are given in Tables I through IV, for both MgO and Al_2O_3 at the two temperature at which the isobaric experiments were performed.

TABLE I. Correction terms in the calculation of $(\partial B_T/\partial P)_T$.

PARAMETER	SYMBOL	VALUE	UNITS
Adiabatic P. deriv. of B	$(\partial B_S/\partial P)_T$	3.916	
Volume expansivity	α	31.4×10^{-6}	
Specific heat	C_p	9.41×10^{6}	erg/gm/°C
Adiabatic compressibility	χ_S	5.824×10^{-13}	cm^2/dyne
Thermal Gruneisen constant	γ	1.585	
Isothermal compressibility	χ_T	5.913×10^{-13}	cm^2/dyne
Temp. deriv. bulk modulus	$(\partial B_T/\partial T)_P$	0.291	kbar/°K
Temp. deriv. expansivity	$(\partial\alpha/\partial T)_P$	1×10^{-7}	
Adiabatic-isothermal corr.	$1+\alpha\gamma T$	1.0153	
Coefficient of [A-B], Eq. (11)	$\alpha\gamma T(C_V/C_p)$	0.0151	
Value of A, Eq. (11)	$2(\alpha B_T)^{-1}(\partial B_T/\partial T)_P$	-10.96	
Value of D, Eq. (11)	$\alpha^{-2}(\partial\alpha/\partial T)_P$	103	
2nd term of Eq. (11)		0.044	
3rd term of Eq. (11)		-0.022	
Isothermal P. deriv. of B	$(\partial B_T/\partial P)_T$	3.94	

TABLE II. Corrections for computing $(\partial B_T/\partial P)$ of MgO at -78.5°C

PARAMETER	SYMBOL	VALUE	UNITS
*P. deriv. adiabatic, B_S	$(\partial B_S/\partial P)_T$	4.00	
*Vol. expansivity	α_v	22.08×10^{-6}	$°C^{-1}$
*Specific heat	C_p	6.37×10^{6}	erg/gm/°C
*adiabatic compressibility	χ_S	5.7823×10^{-13}	cm^2/gm
†Gruneisen constant	γ	1.67	
†Isothermal compressibility	χ_T	5.8238×10^{-13}	cm^2/gm
*T. deriv., bulk modulus	$(\partial B_T/\partial T)_P$	-0.25	kbar/°K
*T. deriv., expansivity	$(\partial \alpha_v/\partial T)_P$	1.3×10^{-7}	
†Adiabatic-isothermal corr.	$1+\alpha_v\gamma T$	1.00717	
†Coeff.: 2nd term, Eq. (11)	$\alpha_v\gamma T(C_V/C_p)$	7.11×10^{-3}	
†2nd term of 2nd term, Eq. (11)	$2(\alpha B_T)^{-1}(\partial B_T/\partial T)_P$	-12.9	
†3rd term of 3rd term, Eq. (11)	$\alpha_v^{-2}(\partial \alpha_v/\partial T)_P$	266	
†Total 2nd term, Eq. (11)		0.034	
†Total 3rd term, Eq. (11)		-0.013	
†Isothermal P deriv., bulk mod.	$(\partial B_T/\partial P)_T$	4.02	

*Measured
†Calculated

TABLE III. Corrections for computing $(\partial B_T/\partial P)$ of Al_2O_3 at 25°C.

PARAMETER	SYMBOL	VALUE	UNITS
*Adiabatic P. deriv., B_S	$(\partial B_S/\partial P)_T$	3.98	
*Vol. expansivity	α	16.32×10^{-6}	$°C^{-1}$
*Specific heat	C_p	7.831×10^{6}	erg/gm/°C
*Adiabatic compressibility	χ_S	3.967×10^{-13}	cm^2/gm
†Gruneisen const.	γ	1.323	
†Isothermal compressibility	χ_T	3.993×10^{-13}	cm^2/gm
*T. deriv., bulk modulus	$(\partial B_T/\partial T)_P$	0.207	kbar/°K
*T. deriv., expansivity	$(\partial\alpha/\partial T)_P$	1.61×10^{-8}	
†Adiabatic-isothermal corr.	$1+\alpha\gamma T$	1.006437	
†Coeff.; 2nd term	$\alpha\gamma T(C_V/C_p)$	6.395×10^{-3}	
†2nd term of 2nd term, Eq. (11)	$2(\alpha B_T)^{-1}(\partial B_T/\partial T)_P$	-10.129	
†3rd term of 3rd term, Eq. (11)	$\alpha^{-2}(\partial\alpha/\partial T)_P$	60.44	
†Total 2nd term, Eq. (11)		0.012	
†Total 3rd term, Eq. (11)		-0.002	
†Isothermal P. deriv., bulk mod.	$(\partial B_T/\partial P)_T$	3.99	

*Measured
†Calculated

TABLE IV. Corrections for computing $(\partial B_T/\partial P)$ of Al_2O_3 at -78.5°C.

PARAMETER	SYMBOL	VALUE	UNITS
*Volume expansivity	α	9.21×10^{-6}	
*P. deriv., adiabatic, B_s	$(\partial B_s/\partial P)_T$	4.00	
*Specific heat	C_p	4.816×10^{6}	erg/gm/°C
*Compressibility, adiabatic	χ_s	3.9460×10^{-13}	cm^2/gm
†Gruneisen constant	γ	1.226	
†Isothermal compressibility	χ_T	3.9547×10^{13}	cm^2/gm
*T. deriv., bulk mod.	$(\partial B_T/\partial T)_P$	0.1284	kbar/°K
*T. deriv., expansivity	$(\partial\alpha/\partial T)_P$	2.73×10^{-8}	
†Adiabatic-isothermal corr.	$1+\alpha\gamma T$	1.002213	
†Coeff.; 2nd term Eq. (11)	$\alpha\gamma T(C_V/C_p)$	2.208×10^{-3}	
†2nd term of 2nd term, Eq. (11)	$2(\alpha B_T)^{-1}(\partial B_T/\partial T)_P$	-11.02	
†3rd term of 3rd term, Eq. (11)	$\alpha^{-2}(\partial\alpha/\partial T)_P$	321.8	
†Total 2nd term, Eq. (11)		0.007	
†Total 3rd term, Eq. (11)		0.006	
†Isothermal P. deriv. bulk mod.	$(\partial B_T/\partial P)_T$	4.01	

*Measured
†Calculated

REFERENCE

1. Overton, W. C., Jr., Relation between ultrasonically measured properties and the coefficients in the solid equation of state, J. Chem. Phys., 37[1], 116-119, 1962.

APPENDIX D

EXPERIMENTAL DATA

The measurements involve the determination of (time^{-1}), a pseudo-resonant frequency, and the frequency ratio as outlined in Appendix B. Here, the data obtained in the course of the experiments and the data employed in subsequent computations are presented.

A. MgO

The length of the MgO specimen used was 0.66924 cm and the bulk density 3.5803 at 25°C. The initial velocities were $v_p = 9.7711$ and $v_s = 5.9682$ as determined at 25°C and 1 atm.

Runs at 1 atm and temperatures from 80°C to -78.5°C (the sublimation temperature of dry ice) were performed and the velocities determined as a function of temperature. The data for these runs are given in Table I. The value of ℓ_o/ℓ was obtained from the thermal expansion data of MgO. This has been evaluated by White and Anderson,[1] based on the work of Ganesan,[2] Sharma,[3] and Skinner.[4]

Variation of the velocities with pressure at constant temperature were performed at +34.6°C and -78.5°C. The vessel was thermostated with a heater at +34.6°C and with dry ice at -78.5°C. The data and velocities obtained are

TABLE I. Longitudinal and Shear Velocities with Temperature at 1 atm for MgO.

Temp. °C	ℓ_0/ℓ	Frequency Ratio Long.	Shear	Velocity (km/sec) Long.	Shear
-80	0.999046	1.005744	1.008665	9.8186	6.0145
-78.5	0.999057	1.005669	1.008591	9.8179	6.0139
-70	0.999120	1.005232	1.008083	9.8143	6.0109
-60	0.999200	1.004715	1.007340	9.8100	6.0069
-50	0.999282	1.004193	1.006520	9.8057	6.0027
-40	0.999368	1.003663	1.005666	9.8014	5.9982
-30	0.999457	1.003115	1.004835	9.7969	5.9938
-20	0.999549	1.002555	1.003987	9.7924	5.9893
-10	0.999644	1.001981	1.003130	9.7877	5.9847
0	0.999742	1.001401	1.002251	9.7830	5.9801
10	0.999843	1.000819	1.001365	9.7783	5.9754
20	0.999947	1.000234	1.000460	9.7736	5.9706
25	1.000000	1.000000	1.000000	9.7711	5.9682
30	1.000053	0.999691	0.999546	9.7686	5.9658
40	1.000159	0.999072	0.998638	9.7636	5.9610
50	1.000268	0.998453	0.997730	9.7586	5.9562
60	1.000378	0.997834	0.996822	9.7536	5.9515
70	1.000491	0.997215	0.995914	9.7487	5.9467
80	1.000604	0.996597	0.995006	9.7437	5.9420

listed in Table II. Table III lists the variation of bulk modulus with pressure computed from these data at the two temperatures.

B. Al_2O_3

The experiments on Al_2O_3 parallel those for MgO. The length of the Al_2O_3 specimen used was 1.2540 cm and the bulk density 3.972 g/cm^2 at 25°C. The initial velocities were determined to be 10.845 km/sec for the longitudinal velocity and 6.3730 km/sec for the shear velocity.

The variation of velocity with temperature as determined from 25°C to -78.5°C is given in Table IV. The thermal expansion data of Wachtman[5] was employed.

Table V lists the velocity data obtained for Al_2O_3 as a function of pressure at constant temperature. Table VI lists the bulk modulus as a function of pressure at the two temperatures.

TABLE II. Longitudinal and shear velocities with pressure at -78.5°C and 34.6°C.

Pressure bars	ℓ_o/ℓ	Frequency Ratio Long.	Shear	Velocity (km/sec) Long.	Shear
34.6°C					
1	1.0000000	1.000000	1.000000	9.7662	5.9635
500	1.0000973	1.000492	1.000463	9.7700	5.9657
1000	1.0001946	1.000985	1.000927	9.7739	5.9679
1500	1.0002919	1.001478	1.001390	9.7778	5.9700
2000	1.0003892	1.001970	1.001853	9.7816	5.9722
2500	1.0004865	1.002463	1.002317	9.7855	5.9744
3000	1.0005838	1.002955	1.002780	9.7893	5.9766
3500	1.0006811	1.003448	1.003243	9.7932	5.9787
4000	1.0007784	1.003940	1.003706	9.7970	5.9809
-78.5°C					
1	1.0000000	1.000000	1.000000	9.8179	6.0139
500	1.0001096	1.000496	1.000451	9.8216	6.0158
1000	1.0002192	1.000992	1.000903	9.8254	6.0179
1500	1.0003288	1.001488	1.001355	9.8292	6.0199
2000	1.0004383	1.001984	1.001806	9.8330	6.0220

TABLE III. Variation of adiabatic bulk modulus with pressure at 34.6°C and -78.5°C for MgO.

Pressure (bars)	Density		Bulk Modulus (kbars)	
	34.6°C	-78.5°C	34.6°C	-78.5°C
1	3.5792	3.5903	1716.7	1729.4
500	3.5802	3.5914	1719.7	1731.4
1000	3.5813	3.5926	1720.5	1733.5
1500	3.5823	3.5938	1722.6	1735.6
2000	3.5834	3.5939	1724.5	1737.6
2500	3.5844		1726.4	
3000	3.5855		1728.4	
3500	3.5865		1730.4	
4000	3.5875		1732.3	

TABLE IV. Longitudinal and shear velocity as function of temperature at 1 atm.

Temp. °C	ℓ/ℓ_o	Frequency Ratio Long.	Shear	Velocity (km/sec) Long.	Shear
25	1.000000	1.000000	1.000000	10.845	6.3730
20	0.999985	1.000186	1.000272	10.847	6.3746
10	0.999929	1.000567	1.000807	10.850	6.3777
0	0.999879	1.000946	1.001332	10.854	6.3807
-10	0.999830	1.001320	1.001847	10.857	6.3837
-20	0.999782	1.0016[illegible]	1.002362	10.861	6.3866
-30	0.999736	1.002[illegible]0	1.002872	10.864	6.3896
-40	0.999697	1.002423	1.003367	10.868	6.3925
-50	0.999657	1.002771	1.003857	10.871	6.3954
-60	0.999619	1.003097	1.004327	10.874	6.3981
-70	0.999583	1.003418	1.004749	10.877	6.4006
-78.5	0.999554	1.003680	1.005080	10.8799	6.40251
-80	0.999549	1.003722	1.005138	10.880	6.4028

TABLE V. Longitudinal and shear velocity as function of pressure at 25°C and -78.5°C.

Pressure (bars)	ℓ_0/ℓ	Frequency Ratio Long.	Shear	Velocity (km/sec) Long.	Shear
25°C					
1	1.0000000	1.000000	1.000000	10.845	6.3730
500	1.0000658	1.000305	1.000239	10.848	6.3741
1000	1.0001325	1.000611	1.000479	10.850	6.3752
1500	1.0001982	1.000917	1.000719	10.853	6.3763
2000	1.0002648	1.001223	1.000958	10.855	6.3774
2500	1.0003304	1.001528	1.001198	10.858	6.3785
3000	1.0003969	1.001834	1.001438	10.861	6.3796
3500	1.0004624	1.002140	1.001677	10.863	6.3807
4000	1.0005300	1.002446	1.001917	10.866	6.3818
-78.5°C					
1	1.0000000	1.000000	1.000000	10.8799	6.40251
500	1.0000656	1.000300	1.000230	10.883	6.4035
1000	1.0001317	1.000600	1.000461	10.885	6.4046
1500	1.0001973	1.000900	1.000691	10.888	6.4057
2000	1.0002632	1.001200	1.000922	10.890	6.4067
2500	1.0003287	1.001499	1.001152	10.893	6.4078
3000	1.0003947	1.001799	1.001383	10.895	6.4088
3500	1.0004601	1.002099	1.001613	10.898	6.4099
4000	1.0005254	1.002399	1.001844	10.900	6.4109

TABLE VI. Variation of Adiabatic Bulk Modulus with pressure at 25°C and -78.5°C for Al_2O_3.

Pressure (bars)	Density (gms/cm^3) 25°C	-78.5°C	Bulk Modulus (kbars) 25°C	-78.5°C
1	3.9720*	3.9773	2520.6	2534.2
500	3.9728	3.9781	2522.5	2535.8
1000	3.9736	3.9789	2524.5	2538.1
1500	3.9744	3.9797	2526.5	2540.1
2000	3.9752	3.9804	2528.5	2542.1
2500	3.9759	3.9812	2530.5	2544.1
3000	3.9767	3.9820	2532.5	2546.1
3500	3.9775	3.9828	2534.5	2548.1
4000	3.9783	3.9836	2536.5	2550.1

*Value of ρ = 3.972 at 25°C and 1 atm is assumed to be exact for the purpose of this calculation.

REFERENCES

1. White, G., and O. L. Anderson, The Gruneisen parameter of magnesium oxide, J. Appl. Phys., in press.

2. Ganesan, S., Temperature variation of the Gruneisen constant parameter in magnesium oxide, Phil. Mag., 7[2], 197-205, 1962.

3. Sharma, S. S., Thermal expansion of crystals. IV Silver chloride, lithium fluoride and magnesium oxide, Proc. Ind. Acad. Sci., 32, 268-274, 1950.

4. Skinner, B. J., Thermal expansion of thoria, periclase and diamond, Am. Min., 42[1-2], 39-55, 1957.

5. Wachtman, J. B., Jr., T. G. Scuderi, and G. W. Cleek, Linear thermal expansion of aluminum oxide and thorium oxide from 100 to 1100°K, J. Am. Ceram. Soc., 45[7], 319-323, 1962.

UNCLASSIFIED

Security Classification

DOCUMENT CONTROL DATA - R&D

(Security classification of title, body of abstract and indexing annotation must be entered when the overall report is classified)

1. ORIGINATING ACTIVITY *(Corporate author)*

Lamont Geological Observatory of Columbia University, Palisades, New York

2a. REPORT SECURITY CLASSIFICATION

UNCLASSIFIED

2b. GROUP

3. REPORT TITLE

Measurement of P and S Sound Velocities under Pressure on Laboratory Models of the Earth's Mantle

4. DESCRIPTIVE NOTES *(Type of report and inclusive dates)*

Final Report, 16 December 1963 - 15 December 1965

5. AUTHOR(S) *(Last name, first name, initial)*

Anderson, Orson L.
Schreiber, Edward

6. REPORT DATE	7a. TOTAL NO. OF PAGES	7b. NO. OF REFS
16 December 1965	74	24

8a. CONTRACT OR GRANT NO.	9a. ORIGINATOR'S REPORT NUMBER(S)
AF-AFOSR 49(638)-1355 b. PROJECT NO. 4810 & 3810 c. Task 8652 d. ARPA Order No. 292-63, 292-64	9b. OTHER REPORT NO(S) *(Any other numbers that may be assigned this report)*

10. AVAILABILITY/LIMITATION NOTICES

11. SUPPLEMENTARY NOTES	12. SPONSORING MILITARY ACTIVITY
	Advanced Research Projects Agency ARPA Order No. 292-63, 292-64

13. ABSTRACT

The techniques of ultrasonic interferometry were used to measure the isotropic sound velocities and their derivatives for polycrystalline specimens of aluminum oxide and magnesium oxide. The pressure derivatives were determined to 4 kbars at room temperature and at -78.5°C. The temperature derivatives were measured at 1 atm. The isothermal pressure derivatives of the bulk modulus and the isothermal temperature derivatives of the bulk modulus were determined. From these data, the critical temperature gradient for velocities, $(dT/dP)_V$, were evaluated, and the velocity behavior of these materials as a function of temperature and depth in the mantle, are discussed. It was found that, because $(dT/dP)_{V_p} > (dT/dP)_{V_s}$, they exhibit a shear velocity minimum and a less pronounced longitudinal velocity minimum under conditions likely to exist in the upper mantle. An expression was derived, employing the measured values of the bulk modulus B_o and its pressure derivative B_o', which predicts compression at extremely high pressures. Using the derived expression $\ell n(V_o/V)=[1/B_o' \ell n(P/B_o)+1]$ and the values of B_o and B_o' for MgO and Al_2O_3 reported here, the agreement between the calculated compression and measured compression reported in the literature was within 0.5% to 350 kilobars.

DD FORM 1 JAN 64 1473

UNCLASSIFIED

Security Classification

14. KEY WORDS	LINK A		LINK B		LINK C	
	ROLE	WT	ROLE	WT	ROLE	WT
Polycrystalline MgO						
Polycrystalline Al_2O_3						
Ultrasonic Interferometry Techniques						
Isotropic Sound Velocities						
Bulk Modulus						
Shear Velocity						
Longitudinal Velocity						
Upper Mantle						
Pressure Derivatives						
Temperature Derivatives						
Calculation of Compressibility						

INSTRUCTIONS

1. ORIGINATING ACTIVITY: Enter the name and address of the contractor, subcontractor, grantee, Department of Defense activity or other organization *(corporate author)* issuing the report.

2a. REPORT SECURITY CLASSIFICATION: Enter the overall security classification of the report. Indicate whether "Restricted Data" is included. Marking is to be in accordance with appropriate security regulations.

2b. GROUP: Automatic downgrading is specified in DoD Directive 5200.10 and Armed Forces Industrial Manual. Enter the group number. Also, when applicable, show that optional markings have been used for Group 3 and Group 4 as authorized.

3. REPORT TITLE: Enter the complete report title in all capital letters. Titles in all cases should be unclassified. If a meaningful title cannot be selected without classification, show title classification in all capitals in parenthesis immediately following the title.

4. DESCRIPTIVE NOTES: If appropriate, enter the type of report, e.g., interim, progress, summary, annual, or final. Give the inclusive dates when a specific reporting period is covered.

5. AUTHOR(S): Enter the name(s) of author(s) as shown on or in the report. Enter last name, first name, middle initial. If military, show rank and branch of service. The name of the principal author is an absolute minimum requirement.

6. REPORT DATE: Enter the date of the report as day, month, year; or month, year. If more than one date appears on the report, use date of publication.

7a. TOTAL NUMBER OF PAGES: The total page count should follow normal pagination procedures, i.e., enter the number of pages containing information.

7b. NUMBER OF REFERENCES: Enter the total number of references cited in the report.

8a. CONTRACT OR GRANT NUMBER: If appropriate, enter the applicable number of the contract or grant under which the report was written.

8b, 8c, & 8d. PROJECT NUMBER: Enter the appropriate military department identification, such as project number, subproject number, system numbers, task number, etc.

9a. ORIGINATOR'S REPORT NUMBER(S): Enter the official report number by which the document will be identified and controlled by the originating activity. This number must be unique to this report.

9b. OTHER REPORT NUMBER(S): If the report has been assigned any other report numbers *(either by the originator or by the sponsor)*, also enter this number(s).

10. AVAILABILITY/LIMITATION NOTICES: Enter any limitations on further dissemination of the report, other than those imposed by security classification, using standard statements such as:

(1) "Qualified requesters may obtain copies of this report from DDC."

(2) "Foreign announcement and dissemination of this report by DDC is not authorized."

(3) "U. S. Government agencies may obtain copies of this report directly from DDC. Other qualified DDC users shall request through _____."

(4) "U. S. military agencies may obtain copies of this report directly from DDC. Other qualified users shall request through _____."

(5) "All distribution of this report is controlled. Qualified DDC users shall request through _____."

If the report has been furnished to the Office of Technical Services, Department of Commerce, for sale to the public, indicate this fact and enter the price, if known.

11. SUPPLEMENTARY NOTES: Use for additional explanatory notes.

12. SPONSORING MILITARY ACTIVITY: Enter the name of the departmental project office or laboratory sponsoring *(paying for)* the research and development. Include address.

13. ABSTRACT: Enter an abstract giving a brief and factual summary of the document indicative of the report, even though it may also appear elsewhere in the body of the technical report. If additional space is required, a continuation sheet shall be attached.

It is highly desirable that the abstract of classified reports be unclassified. Each paragraph of the abstract shall end with an indication of the military security classification of the information in the paragraph, represented as *(TS), (S), (C), or (U)*.

There is no limitation on the length of the abstract. However, the suggested length is from 150 to 225 words.

14. KEY WORDS: Key words are technically meaningful terms or short phrases that characterize a report and may be used as index entries for cataloging the report. Key words must be selected so that no security classification is required. Identifiers, such as equipment model designation, trade name, military project code name, geographic location, may be used as key words but will be followed by an indication of technical context. The assignment of links, rules, and weights is optional